MAPPING WATER ICE IN LUNAR PERMANENTLY SHADOWED REGIONS USING A TWO-BAND LIDAR.

E. A. Cloutis[1], B. R. Dagdick[1], A. E. Parkinson[1], R. V. Kruzlecky[2], P. Murzionak[2], Y. Gao, and C. I. Underwood. [1]Department of Geography, University of Winnipeg, 515 Portage Avenue, Winnipeg, MB, Canada. [2] MPB Communications Inc., 151 Hymus Boulevard, Pointe Claire, QC, Canada. [3]University of Surrey, Guildford, Surrey GU2 7XH, United Kingdom. e.cloutis@uwinnipeg.ca.

Introduction: Detecting and mapping the distribution of water ice and other volatiles in permanently-shadowed polar regions on the Moon is of scientific interest and considered an important enabler of extended human presence on the Moon.

With support from the Canadian Space Agency and the European Space Agency (SysNova program) we have been pursuing definition of a 12U lunar CubeSat mission that would enable high spatial resolution mapping and detection of water ice in permanently-shadowed regions (PSRs) in the lunar South Pole region [1]. This mission would provide higher spatial resolution than the LRO LOLA (4x44 versus ~50 m) and the Lunar Prospector Neutron Spectrometer (~150 km) [2], and hopefully obviate the issues encountered with direct imaging of polar regions by LOLA [3]. The use of a dual-wavelength lidar would also allow for more unambiguous detection of water ice (as discussed below), complementing results from Lunar Prospector on the presence of enhanced hydrogen in PSRs, and better defining their geographic extent and surficial physical and compositional properties.

Cubesat Preliminary Design: Through a just-completed ESA SysNova concept study, we have defined some preliminary operational characteristics for a 12U lunar CubeSat that could be launched as early as 2019. The proposed orbit would enable mapping of a 300 km diameter region centered on the lunar South Pole in ~13 days from a 20 km nadir orbit.

The main science instruments related to this objective are a dual-frequency lidar: 532 and 1560 nm, which share the optical train to provide co-registered data. They would provide data with a spatial resolution of ~4 x 44 m per point, and an ~1.3 km swath width.

The detectors associated with the lidars could also function in passive reflectance mode, enabling mapping of unshadowed regions at multiple wavelengths. This would be accomplished by "masking" portions of the detectors with selected narrow-pass filters to allow for measurement of (passive) reflectance at specific wavelengths. Tentative wavelengths that are being considered for this application are 280 and 1064 nm. The latter wavelength could also be used as a third lidar wavelength if the frequency-doubled laser for 532 nm imaging is also adapted for active 1064 nm illumination. Since the detectors are sensitive to 532 and 1560 nm, we currently envision conducting passive reflectance measurements at 280, 532, 1064, and 1560 nm.

The 280 nm wavelength capability could allow for more robust quantification of ilmenite concentrations [4]. The additional wavelengths would allow for assessing soil maturity and measuring compositional variations [5].

Laboratory studies of lunar analogues: In order to assess how well the proposed two-wavelength lidar system would be able to detect water ice, we conducted reflectance measurements on a suite of samples that included the NASA JSC-1 lunar mare simulant and the CHENOBI lunar highland simulant. This complements work by other team members on generating realistic simulants of PSR regolith [6]. Both simulants have spectral similarities to lunar regolith: both are red-sloped with weak silicate absorption bands, and the mare simulant is darker than the highland simulant. Reflectance spectra were measured in simulated lidar mode (i=e=0°) for a range of sample types:

Sample ID	***Description***
Highland #1	PSA001a: Fine powder, dense pack; multiple incidence angles
Highland #2	PSA001b: Fine powder, loose pack
Highland #3	PSA001c: Fine powder, dense pack
Highland #4	PSA001d: Fine powder, dense pack with loose powder on top
Highland #5	PSA001e: Coarse powder, regular pack; multiple incidence angles
Highland #6	PSA001f: Unsorted powder, regular pack; multiple incidence angles
Highland #7	PSA001g: Unsorted powder, loose pack
Highland #8	PSA001h: Unsorted powder, dense pack
Highland #9	PSA001i: Unsorted powder, dense pack with loose powder on top
Highland #10	PSA001j: Fine powder, rough surface
Highland #11	PSA001k: Unsorted powder, rough surface
Mare #1	PSA003a: Fine powder, regular pack; multiple incidence angles
Mare #2	PSA003b: Fine powder, loose pack
Mare #3	PSA003c: Fine powder, dense pack
Mare #4	PSA003d: Coarse powder, regular pack
Mare #5	PSA003e: Coarse powder, regular pack; multiple incidence angles
Mare #6	PSA003f: Unsorted powder, regular pack; multiple incidence angles
Mare #7	PSA003g: Unsorted powder, loose pack
Mare #8	PSA003h: Unsorted powder, dense pack
Mare #9	PSA003i: Unsorted powder, dense pack with loose powder on top
Mare #10	PSA003j: Fine powder, rough surface

Mare #11	PSA003k: Unsorted powder, rough surface
Ice	Pure ice
Mare #12	PSA003l: Ice with a thin layer of mare powder
Highland #12	PSA001l: Ice with a thin layer of highland powder
Mare #13	PSA003m: Ice with a thick layer of mare powder
Highland #13	PSA001m: Ice with a thick layer of highland powder
Highland #14	PSA001n: Highland powder with 10 wt.% ice mixed in; multiple incidence angles
Highland #15	PSA001o: Highland powder with 20 wt.% ice mixed in
Highland #16	PSA001p: Highland powder with 30 wt.% ice mixed in; multiple incidence angles
Highland #17	PSA001q: Highland powder with 40 wt.% ice mixed in
Highland #18	PSA001r: Highland powder with 50 wt.% ice mixed in; multiple incidence angles
Mare #14	PSA003n: Mare powder with 10 wt.% ice mixed in; multiple incidence angles
Mare #15	PSA003n: Mare powder with 20 wt.% ice mixed in
Mare #16	PSA003p: Mare powder with 30 wt.% ice mixed in; multiple incidence angles
Mare #17	PSA003q: Mare powder with 40 wt.% ice mixed in
Mare #18	PSA003r: Mare powder with 50 wt.% ice mixed in; multiple incidence angles

++

The spectral results largely conformed to expectations. We have focused our initial analysis on the behavior of the samples at 532 and 1560 nm (**Fig. 1**). We found that the reflectance of pure water ice at 532 nm increases with decreasing particle size [7]. The mare and highland simulants have similar 532/1560 nm ratios that vary somewhat with changes in porosity and grain size. The addition of water ice (i.e., the samples were mixed with varying proportions of water and frozen prior to the spectral measurements) results in increases in this reflectance ratio, but show no systematic change in absolute reflectance at 532 nm. It can be seen that a 50-50 mixture of simulant-water ice has a higher 532/1560 nm ratio than the dry samples. This is due to the fact that the 1560 nm bandpass is located in the region of a moderately strong water ice overtone absorption band [7].

Collectively, these results indicate that the use of both absolute reflectance at 532 nm, as well as the 532/1560 nm reflectance ratio allows for discrimination of water ice-bearing regolith simulants from dry samples, and highland from mare samples. It may also allow for constraints to be placed on the physical state of any surficial ice.

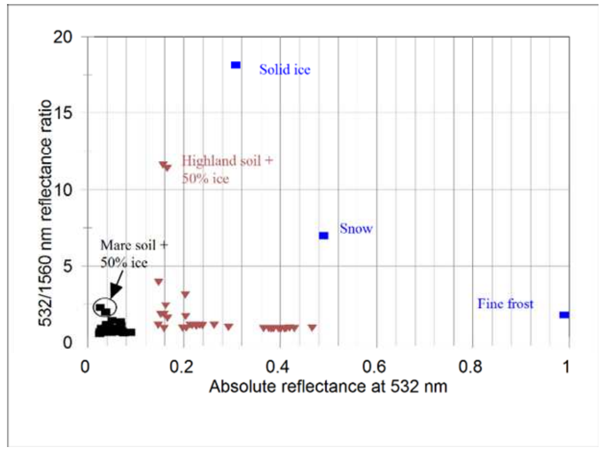

Figure 1. 532/1560 nm reflectance ratio versus absolute reflectance at 532 nm for highland and mare simulants as described above.

Future directions: We will be conducting additional spectroscopic studies that will include additional factors, such as: (1) effects of water ice grain size on regolith surfaces; (2) surficial water ice and frost coatings on regolith; (3) regolith dust on bedrock (dry); (4) variations from normal incidence (local slopes); (5) use of additional lunar regolith simulants. The goal is to gain a better understanding of how the use of this two-lidar system can be used to quantify physical and compositional properties of PSRs, and to enable new approaches to surficial geological mapping using passive spectroscopy, particularly for identification of ilmenite-rich regions.

References: [1] Kruzelecky R.V. et al. (2018) ICES 2018. [2] Feldman W. C. et al. (2001) *JGR*, *106*, 23231-23251. [3] Fisher E. A. et al. (2017) *Icarus*, *292*, 74-85. [4] Staid M.I. and Pieters C.M. (2000) Icarus, 145, 122-139. [5] Lemelin M. et al. (2013) *JGR*, *118*, 2582-2593. [6] Pitcher C. et al. (2016) Adv. Space Res., 57, 1197-1208. [7] Clark R.N. (1986) *JGR*, *86*, 3087-3096.

Acknowledgements: We thank the Canadian Space Agency and European Space Agency SysNova program for supporting ongoing study of the lunar CubeSat concept. We also wish to thank the Canadian Space Agency, the Natural Sciences and Engineering Research Council of Canada, the Canada Foundation for Innovation, the Manitoba Research Innovation Fund, and the University of Winnipeg for supporting establishment and continued operation of the Planetary Spectrophotometer Facility, and this study.